Available online at www.sciencedirect.com
SCIENCE DIRECT®
Journal of Magnetic Resonance 163 (2003) 114–120
JMR Journal of Magnetic Resonance
www.elsevier.com/locate/jmr

Determination of three-bond scalar coupling between $^{13}C'$ and $^{1}H^{\alpha}$ in proteins using an iHN(CA),CO(α/β-*J*-COHA) experiment

Perttu Permi*

NMR Laboratory, Structural Biology and Biophysics, Institute of Biotechnology, P.O. Box 65, University of Helsinki, Helsinki FIN-00014, Finland

Received 5 December 2002; revised 19 February 2003

Abstract

Triple-resonance NMR experiments for measuring three-bond scalar coupling constant between $^{13}C'(i-1)$ and $^{1}H^{\alpha}(i)$ spins, defining the dihedral angle ϕ, are presented. The novel experiments enable the measurement of $^{3}J_{C'H^{\alpha}}$ from simple two (or three)-dimensional $^{13}C'$, ($^{15}N/^{13}C^{\alpha}$), $^{1}H^{N}$ correlation spectra with minimal resonance overlap, thanks to solely intraresidual coherence transfer pathway and spin-state-selection. The $^{3}J_{C'H^{\alpha}}$ values measured in human ubiquitin using the proposed intraresidual iHN(CA),CO(α/β-*J*-COHA) TROSY method were compared with those determined previously utilizing the HCAN[C′] experiment.

Keywords: Coupling constants; iHNCA; Spin-state-selective filters; TROSY; Ubiquitin

1. Introduction

Three-bond scalar couplings can be related to Ramachandran angles, ϕ and ψ, defining conformation of polypeptide chain. These relations are based on famous Karplus equations [1,2]. Backbone dihedral ψ is only defined by three ^{3}J-couplings, $^{3}J_{H^{\alpha}N}$, $^{3}J_{NC^{\beta}}$, and $^{3}J_{NN}$ [3–5]. In practice, only $^{3}J_{H^{\alpha}N}$ is useful for determining main-chain angle ψ [4,5]. However, there are six different *J*-couplings, $^{3}J_{H^{N}H^{\alpha}}$, $^{3}J_{H^{N}C'}$, $^{3}J_{H^{N}C^{\beta}}$, $^{3}J_{C'H^{\alpha}}$, $^{3}J_{C'C'}$, and $^{3}J_{C'C^{\beta}}$ which can be used to probe the course of main chain dihedral ϕ through existing Karplus relations [6–10]. The existing repertoire for measuring these ^{3}J couplings is large [6–27], although extensive development of methodology has been carried out only in the case of $^{3}J_{H^{N}H^{\alpha}}$ [17–27]. In this paper we shall focus on measurement of three-bond scalar coupling between $^{13}C'(i-1)$ and $^{1}H^{\alpha}(i)$, ranging from 0 to 8 Hz. This coupling has previously been measured by employing quantitative *J*-correlation [11] as well as E.COSY-type of techniques [28]. Wang and Bax used an HCAN[C′]E.COSY experiment for reparametrization of Karplus curve for the $^{3}J_{C'H^{\alpha}}$ coupling [7]. This experiment requires long magnetization transfer steps from $^{13}C^{\alpha}$ to ^{15}N and back during which the $^{13}C^{\alpha}$ spin remains in transverse plane. Thus, fast transverse relaxation of $^{13}C^{\alpha}$ spin results in considerable loss in sensitivity especially on larger proteins. Löhr and Rüterjans designed an elegant H^{α}-coupled H(N)CA,CO experiment in order to minimize sensitivity losses due to rapid R_2 of $^{13}C^{\alpha}$ spin [15]. In their experiment $^{3}J_{C'H^{\alpha}}$ is determined from an E.COSY pattern in indirectly detected $^{13}C'$ dimension, requiring resolved $^{1}J_{C^{\alpha}H^{\alpha}}$ splitting in the orthogonal $^{13}C^{\alpha}$ dimension. In addition, two sets of cross peaks arise per each residue, potentially inducing resonance overlap. Meissner et al., employed a spin-state-selective filter in their S^3E version of the H(N)CA,CO experiment in order to further diminish time of transverse $^{13}C^{\alpha}$ magnetization as well as to reduce unnecessary spectral crowding due to $^{1}J_{C^{\alpha}H^{\alpha}}$ splitting [14]. Despite of spin-state-selective editing, the S^3E H(N)CA,CO method cannot be recorded as a two-dimensional experiment even in the case of smaller proteins since the sequential cross peaks arising from the

* Fax: +358-9-191-59541.
E-mail address: perttu.permi@helsinki.fi.

1090-7807/03/$ - see front matter © 2003 Elsevier Science (USA). All rights reserved.
doi:10.1016/S1090-7807(03)00079-X

undesired $^{2}J_{NC^{\alpha}}$ transfer will impair the measurement of $^{3}J_{C'H^{\alpha}}$. Even three-dimensional experiment will not afford complete relief to a problem since potential overlap of intra- and interresidual correlations may deteriorate data analysis especially on larger proteins. Another proposed, the $S^{3}P$ HN(CA),CO, experiment potentially facilitates measurement of $^{3}J_{C'H^{\alpha}}$ from two (or three) dimensional spectrum but it hinges on exclusive magnetization transfer from $^{15}N(i)$ to $^{13}C^{\alpha}(i)$ spin, the situation which is not readily obtained using the HNCA-type magnetization transfer [14].

In this paper, we propose novel triple resonance experiments, utilizing recently introduced spin-state-selection technique [29–34] and intraresidual coherence transfer pathway scheme [35]. In this way, we are able to measure $^{3}J_{C'H^{\alpha}}$ couplings from well-dispersed spin-state-selective, two or (three)-dimensional $^{13}C'(i-1)$, ($^{15}N(i)$ or $^{13}C^{\alpha}(i)$), $^{1}H^{N}(i)$ correlation spectrum.

2. Results and discussion

A novel intraresidual HN(CA),CO experiment for measuring $^{3}J_{C'H^{\alpha}}$ is schematically presented in Fig. 1a. The corresponding TROSY [36,37] version of the experiment is shown in Fig. 1b. For simplicity, the density operator description of the methodology is presented for the iHN(CA),CO(α/β-*J*-COHA). The proposed iHN(CA),CO(α/β-*J*-COHA) experiment is based on intraresidual HNCA experiment [35]. The desired coherence floats through the iHN(CA),CO(α/β-*J*-COHA) experiment in a following way:

$$^{1}H^{N} - \{^{1}J_{HN_N}\} - ^{15}N - \{^{1}J_{NC'}, ^{1}J_{NC^{\alpha}}, ^{2}J_{NC^{\alpha}}\} - ^{13}C' - \{^{1}J_{C'C^{\alpha}}\} - ^{13}C^{\alpha}(^{1}J_{C^{\alpha}H^{\alpha}}) - ^{13}C'(t_1) - \{^{1}J_{C'C^{\alpha}}\} - \{^{1}J_{NC'}, ^{1}J_{NC^{\alpha}}, ^{2}J_{NC^{\alpha}}\} - ^{15}N(t_2) - \{^{1}J_{H^{N}N}\} - ^{1}H^{N}(t_3),$$

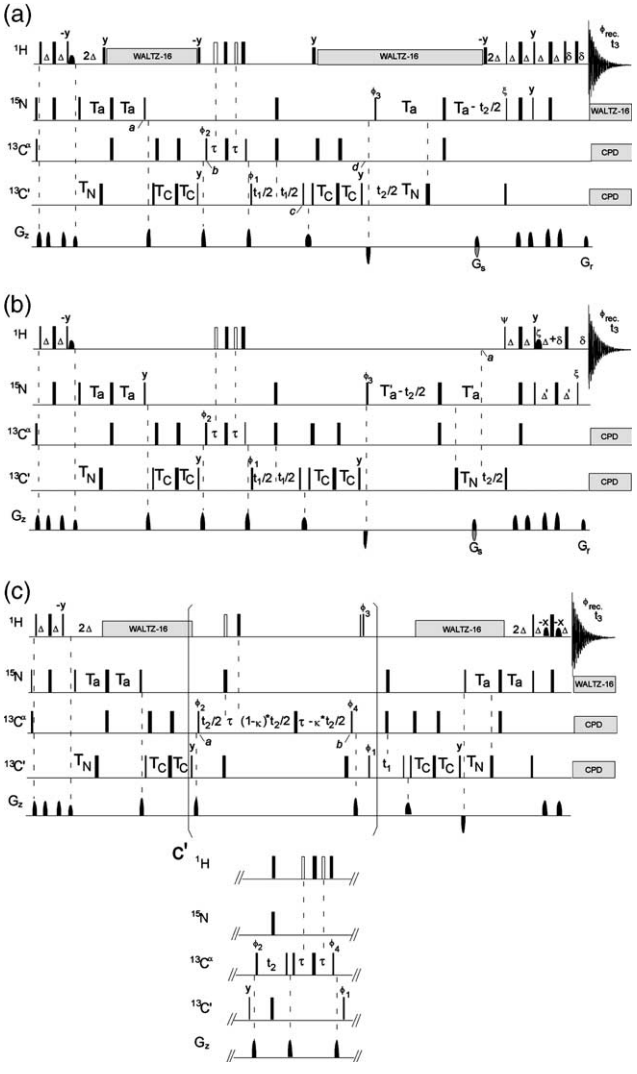

Fig. 1. Pulse sequences for the measurement of $^{3}J_{C'H^{\alpha}}$ couplings in ^{15}N-, ^{13}C-labeled proteins. Narrow (wide) bars correspond to 90° (180°) pulses, with phase *x* unless otherwise indicated. Half-ellipses denote water selective 90° pulses to obtain water-flip-back. All 90° (180°) pulses for $^{13}C'$ and $^{13}C^{\alpha}$ are applied with a strength of $\Omega/\sqrt{15}(\Omega/\sqrt{3})$, where Ω is the frequency difference between the centers of the $^{13}C'$ and $^{13}C^{\alpha}$ regions. The ^{1}H, ^{15}N, $^{13}C'$, and $^{13}C^{\alpha}$ carrier positions are 4.7 (water), 120 (center of ^{15}N spectral region), 175 ppm (center of $^{13}C'$ spectral region), and 55 ppm (center of $^{13}C^{\alpha}$ spectral region), respectively. Pulsed field gradients are inserted as indicated for coherence transfer pathway selection and residual water suppression. The delays employed are: $\Delta = 1/(4J_{NH})$; $\Delta' = \Delta + \delta/2$; $T_a = 25\,\text{ms}$; $T'_a = T_a - \Delta$; $T_N = 1/(4J_{NC'})$; $T_C = 1/(4J_{C'C^{\alpha}})$; $\tau = 1/(4J_{CH})$; $\delta = G_r$ + field recovery delay; $0 \leqslant \kappa \leqslant (\tau)/\ t_{2,\max}$. For each scheme, the in- and antiphase data are recorded in an interleaved manner and subsequently added and subtracted to separate the multiplet components to two subspectra. (a) The iHN(CA),CO(α/β-*J*-COHA) scheme. Phase cycling for the in-phase spectrum: $\phi_1 = x, -x$; $\phi_2 = 2(x)$, $2(-x)$; $\phi_3 = x$; $\xi = x$; $\phi_{rec.} = x, 2(-x), x$; for the antiphase spectrum: $\phi_2 = 2(y), 2(-y)$. Quadrature detection in the F_1-dimension is obtained by altering the phase of ϕ_1 according to States-TPPI [41]. For quadrature detection in F_2, two data sets, both for the in- and antiphase spectra, are collected (I): $\xi = x$; (II): $\xi = -x$ with simultaneous change in gradient polarity [42]. The data processing is according to sensitivity enhanced method [42]. Gradient strengths (durations) are optimized for the highest sensitivity: $G_s = 30\,\text{G/cm}$ (1.25 ms), $G_r = 29.6\,\text{G/cm}$ (0.125 ms). (b) The iHN(CA),CO(α/β-*J*-COHA)-TROSY scheme. All parameters as in (a) except for quadrature detection and TROSY selection in F_2, two data sets, both for the in- and antiphase spectra, are collected (I): $\psi = x$; $\xi = y$; $\zeta = -x$, (II): $\psi = -x$; $\xi = -y$; $\zeta = x$ with simultaneous change in gradient polarity [37]. If removal of the $^{2}J_{N(i)H^{\alpha}(i)}$ coupling during t_2 is desired, an additional 180° (^{1}H) pulse is applied at time point *a* and two data sets collected for the TROSY selection are changed as follows: (I): $\psi = -x$; $\xi = y$; $\zeta = x$, (II): $\psi = x$; $\xi = -y$; $\zeta = -x$. (c) The iH(N)CA,CO(α/β-*J*-COHA) experiment with semi-constant time spin-state-selective filtering scheme. All parameters as in (a) except phase cycling for the in-phase spectrum: $\phi_1 = x, -x$; $\phi_2 = 2(x), 2(-x)$; $\phi_3 = 4(x), 4(-x)$; $\phi_4 = x$; $\phi_{rec.} = x, 2(-x), x$; for the antiphase spectrum: $\phi_4 = y$; $\phi_{rec.} = x, 2(-x), x, -x, 2(x), -x$. Quadrature detection in the F_1 (and F_2)-dimensions is obtained by altering the phase of ϕ_1 (ϕ_2) according to States-TPPI [41]. Alternatively, the iH(N)CA,CO (α/β-*J*-COHA) experiment can be recorded with PFG *z*-filtering scheme (c') using the following phase cycling for the in-phase experiment $\phi_1 = x, -x$; $\phi_2 = 2(x), 2(-x)$; $\phi_4 = x$; $\phi_{rec.} = x, 2(-x), x$. For the antiphase experiment: $\phi_4 = y$.

where t_i ($i = 1$ to 3) is an acquisition time for the corresponding spin and the couplings used for coherence transfer are shown in parenthesis. The spin-state-selective filter element is placed prior to the t_1 evolution period for the purpose of subspectral editing.

In order to survey $^3J_{C'H^\alpha}$, we transfer the $^1H^N$ magnetization to the preceding $^{13}C'(i-1)$ spin, while simultaneously transferring the magnetization to both intra- and interresidual $^{13}C^\alpha$ spins during the delay $2T_a$. The relative density operator at time point a can then be described with the corresponding product operators:

$$\begin{aligned}\sigma_a = {} & 8N_y(i)C'_z(i-1)C^\alpha_z(i-1)C^\alpha_z(i)\sin(2\pi^1 J_{NC^\alpha}T_a)\\ & \times \sin(2\pi^2 J_{NC^\alpha}T_a)\sin(2\pi J_{NC'}T_N) + 2N_y(i)C'_z(i-1)\\ & \times \cos(2\pi^1 J_{NC^\alpha}T_a)\cos(2\pi^2 J_{NC^\alpha}T_a)\sin(2\pi J_{NC'}T_N).\end{aligned}$$

We should point out that the delay $2T_a$ is set to $\sim$50 ms [35]. This will ensure that coherence transfer is maximized for the desired pathway. More importantly, the transfer efficiency will be at least 20 times lower for the undesired pathway provided that $^1J_{NC^\alpha}$ and $^2J_{NC^\alpha}$ are in the range of 9–12 and 6–9 Hz, respectively [35]. For the sake of clarity, let us now omit the undesired magnetization component as well as trigonometric terms and elaborate on the flow of desired $8N_y(i)C'_z(i-1)\ C^\alpha_z(i-1)C^\alpha_z(i)$ coherence. This magnetization is next converted into the $^{13}C'$ single-quantum coherence by the succeeding 90° pulses on ^{15}N and $^{13}C'$. The ensuing $^{13}C' - ^{13}C^\alpha$ INEPT step converts the magnetization into the $^{13}C^\alpha$ single-quantum coherence (time point b)

$$\sigma_b = 4N_z(i)C'_z(i-1)C^\alpha_y(i).$$

At this point, the spin-state-selective half-filter [5], conceptually similar to the S^3P element [14], is inserted into the pulse sequence. Thus, we convert the $4N_z(i)C'_z(i-1)C^\alpha_y(i)$ magnetization, with respect to $^1H^\alpha(i)$ spin, into $8N_z(i)C'_z(i-1)C^\alpha_z(i)H^\alpha_z(i)$ coherence in the first experiment, referred here to as the antiphase experiment. To this end, two 180° (^1H) pulses marked with filled bars are applied immediately before 180° ($^{13}C^\alpha$) and 90 ($^{13}C^\alpha$) pulses, respectively. In addition, the phase of the $90°_{\phi_2}(^{13}C^\alpha)$ pulse is shifted 90° with respect to the succeeding 90° ($^{13}C^\alpha$) pulse. The ensuing gradient pulse purges a dispersive component of magnetization arising from J-mismatch [5]. The $^{13}C'(i-1)$ chemical shift is then recorded during the t_1 evolution period while the small three-bond coupling between the $^{13}C'(i-1)$ and $^1H^\alpha(i)$ spins evolves simultaneously. The magnetization can be described for the antiphase experiment at the end of the t_1 evolution period by the density operator (time point c)

$$\begin{aligned}\sigma_c = {} & 8N_z(i)C'_y(i-1)C^\alpha_z(i)H^\alpha_z(i)\cos(\pi^3 J_{C'(i-1)H^\alpha(i)}t_1)\\ & \times \cos(\omega_{C'(i-1)}t_1) + 4N_z(i)C'_x(i-1)C^\alpha_z(i)\\ & \times \sin(\pi^3 J_{C'(i-1)H^\alpha(i)}t_1)\cos(\omega_{C'(i-1)}t_1)\\ & + 8N_z(i)C'_x(i-1)C^\alpha_z(i)H^\alpha_z(i)\cos(\pi^3 J_{C'(i-1)H^\alpha(i)}t_1)\\ & \times \sin(\omega_{C'(i-1)}t_1) + 4N_z(i)C'_y(i-1)C^\alpha_z(i)\\ & \times \sin(\pi^3 J_{C'(i-1)H^\alpha(i)}t_1)\sin(\omega_{C'(i-1)}t_1).\end{aligned}$$

The ensuing gradient z-filter destroys the undesired components of magnetization, i.e., the second and third term in σ_c. We would like to clarify that it is possible to implement $^{13}C'$ shift and $^3J_{C'H^\alpha}$ coupling evolution periods in a semi-constant time manner [38]. This would, however, require an additional filtering step to get rid off the undesired dispersive magnetization components due to $^1J_{C'C^\alpha}$ mismatch with respect to $2T_C$. After labeling the $^{13}C'(i-1)$ chemical shift with $^3J_{C'H^\alpha}$ frequencies, the magnetization floats back to the amide proton by the same, but reverse coherence transfer pathway. The ^{15}N chemical shift is recorded during the t_2 evolution period, which is implemented into the ^{13}C–^{15}N back-INEPT in the usual constant-time manner.

In the second experiment, referred to as the in-phase experiment, two 180° (^1H) pulses marked with unfilled bars are applied at the midpoint of delays τ in order to retain the desired coherence in-phase with respect to $^1H^\alpha(i)$ spin, i.e., to preserve $4N_z(i)C'_z(i-1)C^\alpha_y(i)$ magnetization prior to the t_1 period. After the t_1 evolution period, the density operator for the in-phase experiment can be given, neglecting dispersive components of magnetization subsequently purged by the PFG z-filter (time point c)

$$\begin{aligned}\sigma_c = {} & 8N_z(i)C'_y(i-1)C^\alpha_z(i)H^\alpha_z(i)\sin(\pi^3 J_{C'(i-1)H^\alpha(i)}t_1)\\ & \times \sin(\omega_{C'(i-1)}t_1) + 4N_z(i)C'_y(i-1)C^\alpha_z(i)\\ & \times \cos(\pi^3 J_{C'(i-1)H^\alpha(i)}t_1)\cos(\omega_{C'(i-1)}t_1).\end{aligned}$$

Ultimately, we transfer the magnetization back to the amide proton as in the antiphase experiment.

After post-acquisitional addition and subtraction of the antiphase and in-phase data sets, we obtain two (three)-dimensional subspectra with correlations appearing at $\omega_{C'}(i-1) + \pi^3 J_{C'H^\alpha}$, $\omega_N(i)$, $\omega_{H^N}(i)$, and $\omega_{C'}(i-1) - \pi^3 J_{C'H^\alpha}$, $\omega_N(i)$, $\omega_{H^N}(i)$, respectively. Hence, $^3J_{C'H^\alpha}$ can be measured from the cross peak displacement in the $^{13}C'$ dimension between two subspectra from the well-dispersed $^{13}C'(i-1)$, $^{15}N(i)$, $^1H^N(i)$ correlation map.

There are numerous aspects to consider in obtaining the optimal performance. First, for larger proteins TROSY version of the experiment (Fig. 1b) should provide higher sensitivity due to relatively long ^{13}C–^{15}N out- and back-INEPT steps. It should be noted that when proton decoupling is omitted during the ^{13}C–^{15}N back-INEPT and if the spin-state of $^1H^\alpha$ is not perturbed between the t_1 and t_3 evolution periods, $^3J_{H^NH^\alpha}$

can be measured in F_3 between two subspectra. However, due to short lifetime of $^1H^\alpha$ spin-state, especially on large proteins, the familiar E.COSY pattern collapses during the long back-transfer step [7]. In practice, the $^3J_{H^NH^\alpha}$ couplings are underestimates of their true values. Analogously, due to small two-bond coupling between the $^1H^\alpha(i)$ and $^{15}N(i)$ spins during t_2 in a three-dimensional TROSY experiment, an E.COSY pattern arises in F_2-dimension, which may impede determination of $^3J_{C'H^\alpha}$ in the orthogonal dimension. If desired, this can be removed by a 180° (^1H) pulse, applied at time point *a* (*see text for* Fig. 1b *for details*). The caveat is that the TROSY effect will be lost for $t_2/2$ period although we can take advantage of it during relatively long ^{15}N–^{13}C transfer periods.

In order to provide highest sensitivity by maintaining TROSY effective throughout the most of the pulse sequence, we purposely employ also two 180° (^1H) pulses during the filter elements [5]. This also suppresses cross-correlation between chemical shielding anisotropy (CSA) of $^{13}C^\alpha$ and dipole–dipole relaxation (DD) of $^{13}C^\alpha$–$^1H^\alpha$ by averaging relaxation rates of doublet components by the inversion of $^1H^{\alpha\prime}$s spin-state during the filter elements [5].

There are different kind of source of errors, potentially leading to inaccurate determination of $^3J_{C'H^\alpha}$. First, the differential relaxation of antiphase $4N_z(i)C'_z(i-1)C^\alpha_y(i)$ and in-phase $8N_z(i)C'_z(i-1)C^\alpha_y(i)H^\alpha_z(i)$ operators between the spin-state-selective filter element and t_1 may lead to insufficient separation of spin-states. This will result in systematically underestimated coupling constants due to the fact that $^3J_{C'H^\alpha}$ is in most cases smaller than the linewidth. However, delay between the filter and the evolution period is kept to a minimum in order to avoid problems arising from differential relaxation [33].

The spin-state-selective filters are sensitive to a J mismatch when coupling evolution does not exactly match the filter period [30–34]. This is deleterious for subspectral editing and may complicate the accurate determination of coupling constants. In this case, the filter is compensated to a first order for the J mismatch. This will not pose to a significant problem since the editing is excellent when $^1J_{CH}$ is in the 120–170 Hz range [5]. It is noteworthy that the spin-state-selective filter can be replaced by the DIPSAP element [39] for more efficient filtering performance, albeit with a significant cost in sensitivity. In general, effects of J crosstalk on accuracy of measured couplings, as well as its removal, has been discussed earlier [30–34,39].

The final source of error is incomplete elimination of magnetization transfer pathway yielding sequential cross peak. As long as there is no frequency separation in $^{13}C^\alpha$ dimension, there is now way we can tell whether complete elimination of interresidual pathway has emerged. Thus, in the case of $\omega_{C'}(i-1)$, $\omega_N(i)$, $\omega_{H^N}(i)$ correlation map, the sequential pathway is superimposed with the desired intraresidual pathway due to lack of frequency separation in the $^{13}C^\alpha$ dimension. However, the transfer efficiency of the intraresidual pathway will be at least 20 times higher than for the undesired sequential pathway provided that $^1J_{NC^\alpha}$ and $^2J_{NC^\alpha}$ are in the range of 9–12 and 6–9 Hz, respectively [35]. Typically the suppression of the undesired, sequential pathway is excellent. The sequential pathway can be completely removed by recording two data sets with and without an additional 90° ($^{13}C^\alpha$) pulse applied at time point d while inverting receiver phase between the data sets [35]. The relevant product operators at time point d are

$$\sigma_d = 2N_z(i)C'_z(i-1) + 8N_z(i)C'_z(i-1)C^\alpha_z(i-1)C^\alpha_z(i).$$

The 90° ($^{13}C^\alpha$) pulse operates only for the latter term in the first data set while both terms are left intact in the second data set. Therefore, by subtracting these data sets, the first term can be eliminated. The caveat using this active suppression of sequential pathway is a loss of sensitivity by the factor of $\sqrt{2}$. Another, but only partial, solution to the problem is to record $^{13}C^\alpha$ chemical shift instead of ^{15}N. The pulse sequence for this iH(N)CA,CO(α/β-*J*-COHA) experiment is shown in Fig. 1c. It is essentially similar to the iHN(CA),CO(α/β-*J*-COHA) experiment except that we label the $^{13}C^\alpha$ chemical shift during t_2 instead of ^{15}N. Additionally, the iHN(CA),CO(α/β-*J*-COHA) experiment utilizes a novel filter element for separation of α- and β-spin-states, which will be shortly described. In order to reduce the time $^{13}C^\alpha$ spin being in transverse plane, the t_2 evolution period is concatenated with the spin-state selective filter (Fig. 1c, time points *a*–*b*). It is possible to implement the $^{13}C^\alpha$ chemical shift evolution in a semi-constant time manner, since $^{13}C^\alpha$–$^1H^\alpha$ spin–spin interaction is active during 2τ, whereas it is effectively decoupled during t_2. Again, the antiphase data set is recorded with 180° (^1H) pulse (denoted by filled bar) placed after $t_2/2+\tau$, whereas the in-phase data is obtained by inserting the 180° (^1H) pulse (unfilled bar) after $t_2/2$. The clean selection of the desired in- or antiphase coherences with respect to the $^1H^\alpha(i)$ spin is obtained by two consecutive 90° (^1H) pulses (time point *b*) in a manner similar to the famous X-half filter [40]. Alternatively, the spin-state selection can be accomplished utilizing the filtering scheme analogous to one implemented in the iHN(CA),CO(α/β-*J*-COHA) experiment as depicted in Fig. 1c'.

Hence, correlations arise at $\omega_{C^\alpha}(i)+\omega_{C'}(i-1)+\pi^3J_{C'H^\alpha}$, $\omega_{H^N}(i)$, and $\omega_{C^\alpha}(i)+\omega_{C'}(i-1)-\pi^3J_{C'H^\alpha}$, $\omega_{H^N}(i)$ after addition and subtraction of antiphase and in-phase data sets. Now, the intra- and sequential cross peaks from the residues exhibiting peculiar $^1J_{NC^\alpha}$ and/or $^2J_{NC^\alpha}$ couplings can be separated in $^{13}C^\alpha$ dimension in the case of incomplete suppression of sequential

pathway, i.e., the undesired sequential connectivities would emerge at $\omega_{C^\alpha}(i-1)+\omega_{C'}(i-1)+\pi^2 J_{C'H^\alpha}$, $\omega_{H^N}(i)$, and $\omega_{C^\alpha}(i-1)+\omega_{C'}(i-1)-\pi^2 J_{C'H^\alpha}$, $\omega_{H^N}(i)$. However, the sensitivity enhancement scheme cannot be applied to $^{13}C^\alpha$ dimension resulting in sensitivity loss by $\sqrt{2}$ in comparison with the iHN(CA),CO(α/β-*J*-COHA) scheme. In addition, this experiment has to be recorded as three-dimensional experiment.

Therefore, if it is desired to ensure complete suppression of sequential pathway, it is more judicious to utilize the iHN(CA),CO(α/β-*J*-COHA) experiment with active suppression of sequential pathway. The iHN(CA),CO(α/β-*J*-COHA) scheme provides not only higher sensitivity (semi-constant time $^{13}C^\alpha$ evolution vs. constant time ^{15}N evolution) but it can also be recorded as a two-dimensional $^{13}C'(i-1)$, $^1H^N(i)$ correlation experiment.

The sensitivity of the experiments is mainly limited by the transverse relaxation time of ^{15}N spin owing to longer ^{15}N to ^{13}C transfer step in comparison with the familiar HN(CO)CA method for instance. It is then obvious that TROSY version of the experiment is mandatory for larger proteins. We presume that the proposed methodology is applicable to smaller and medium-sized proteins, or proteins, for which perdeuteration is not required.

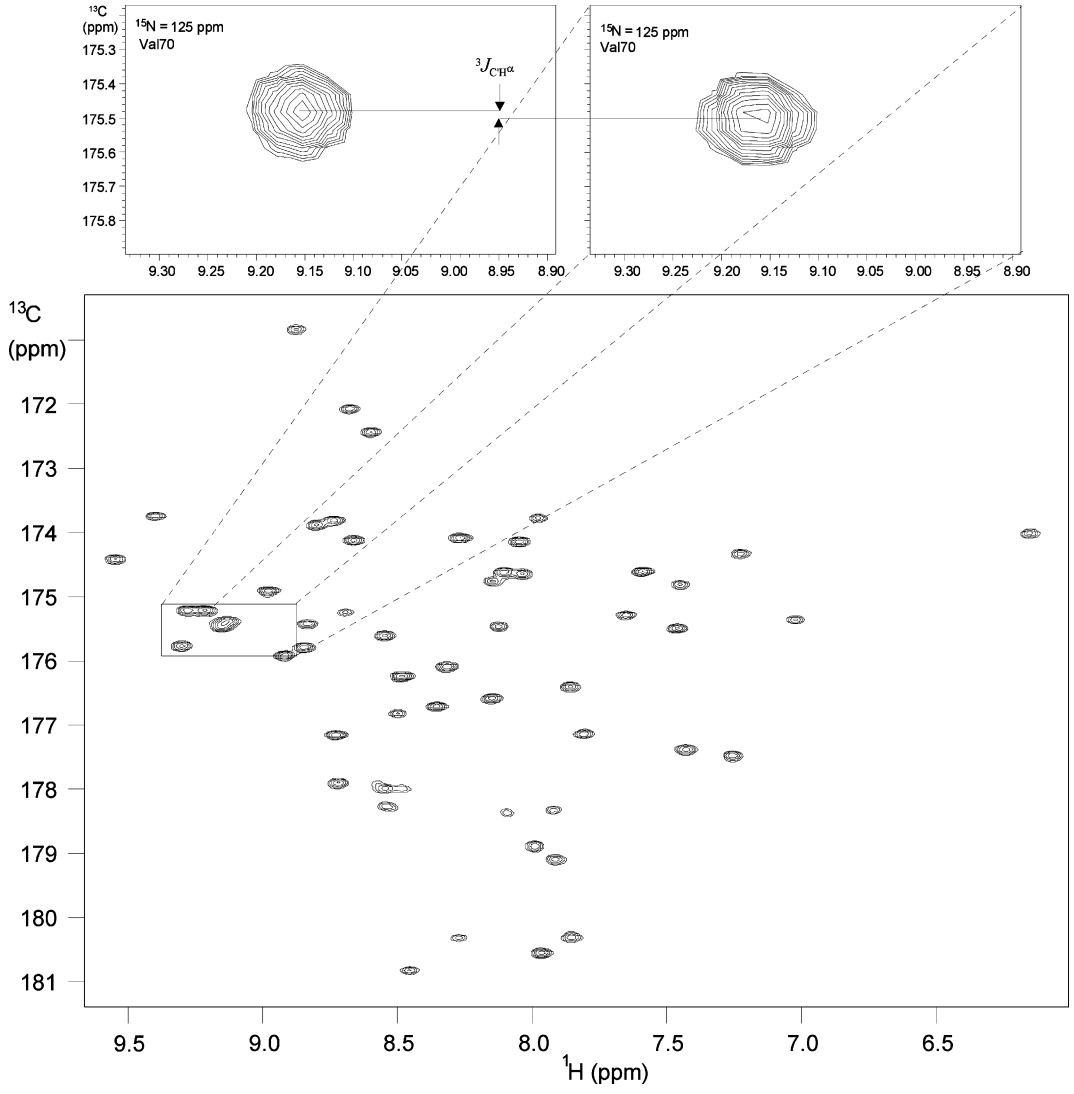

Fig. 2. Two-dimensional iHN(CA),CO(α/β-*J*-COHA)-TROSY subspectrum, recorded from 0.58 mM U-(^{15}N, ^{13}C) ubiquitin, 95/5% H_2O/D_2O, 30 °C at 600 MHz ^1H frequency. Inserted expansions show $^{13}C'$–$^1H^N$ planes from three-dimensional iHN(CA),CO(α/β-*J*-COHA)-TROSY subspectra for Val70 residue. The $^3J_{C'H^\alpha}$ can be measured from cross peak displacement between subspectra in F_1-dimension whereas $^3J_{H^NH^\alpha}$ can be obtained in F_3. Asymmetry in cross peaks arises from $^1H^\alpha$ spin flips during lengthy (~57 ms) from ^{13}C back to $^1H^N$ transfer steps. Therefore measured $^3J_{H^NH^\alpha}$ couplings are underestimates of their true values. Two-dimensional data were zero-filled to 1024 × 4096 data matrix whereas three-dimensional spectrum was zero-filled to 1024 × 128 × 1024 data matrix. The spectra were apodized with shifted squared sine-bell functions in all dimensions.

The viability of the proposed iHN(CA),CO(α/β-*J*-COHA) method for the measurement of the $^{3}J_{H^{\alpha}(i)-C'(i-1)}$ scalar couplings was verified on a 0.58 mM uniformly $^{15}N/^{13}C$ enriched human ubiquitin, (Asla, Riga, Latvia) having a molecular mass of 8.6 kDa (76 amino acid residues), dissolved in 95/5% H_2O/D_2O, 10 mM potassium phosphate buffer, pH 7.2, in a 260 μl Shigemi microcell at 30 °C. The three-dimensional iHN(CA),CO(α/β-*J*-COHA)-TROSY experiment (without active suppression of sequential pathway) was carried out on a Varian Unity INOVA 600 NMR spectrometer, equipped with a $^{15}N/^{13}C/^{1}H$ triple-resonance probehead and an actively shielded *z*-axis gradient coil. The spectrum was acquired as a three-dimensional experiment using four transients per FID with 128, 30, and 1024 complex points and the corresponding acquisition times of 64, 18.8, and 128 ms in t_1, t_2, and t_3, respectively. The employed delays were $T_a = 25$ ms, $T_N = 16.6$ ms, $T_C = 4.55$ ms, $\Delta = 2.75$ ms, $\tau = 1.7$ ms, $\delta =$ gradient + field recovery delay. The data were zero-filled to $1024 \times 128 \times 1024$ matrix before Fourier transform and phase-shifted squared sine-bell window functions were applied in all dimensions. In addition, two-dimensional $^{13}C'$–$^{1}H^{N}$ correlation experiment was recorded with 128 and 1024 complex points in t_1 and t_3, using 64 transients.

Fig. 2 illustrates one of the two-dimensional $^{13}C'$–^{1}H subspectra recorded with the pulse scheme shown in Fig. 1b. Cross peaks represent $\omega_{C'}(i-1) + \pi^{3}J_{C'H^{\alpha}}$, $\omega_{H^{N}}(i)$ correlations. As can be seen, some of the cross peaks are overlapping although very good dispersion can be expected for the $^{1}H^{N}$–$^{13}C'$ correlation spectrum. Expansions of the overlapping region in Fig. 2 depicts two 3D subspectra, exhibiting correlations at $\omega_{C'}(i-1) + \pi^{3}J_{C'H^{\alpha}}$, $\omega_{N}(i)$, $\omega_{H}N(i)$ and $\omega_{C'}(i-1) - \pi^{3}J_{C'H^{\alpha}}$, $\omega_{N}(i)$, $\omega_{H^{N}}(i)$ from Val70 residue. Three-dimensional subspectra were obtained by adding and subtracting the antiphase and in-phase data sets, acquired with the pulse scheme shown in Fig. 1b (without active suppression of sequential pathway) in an interleaved manner. The relevant $^{3}J_{C'H^{\alpha}}$ coupling can be readily measured from the $^{13}C'$ dimension between correlations arising in two subspectra. In addition, $^{3}J_{H^{N}H^{\alpha}}$ coupling could be measured from $^{1}H^{N}$ dimension thanks to the E.COSY pattern arising in F_1–F_3 plane. In practice, however, the measured coupling is an underestimate of true $^{3}J_{H^{N}H^{\alpha}}$ due to long ^{13}C–^{15}N back transfer step.

Fifty-four $^{3}J_{C'H^{\alpha}}$ couplings were measured for ubiquitin, excluding 6 glycines and 3 prolines, from a 3D-spectra collected in 45 h. In addition, residues 7–12 and 74–76 were not observed due to chemical exchange broadening. The measured couplings vary between 0.5 and 7.9 Hz. The residues residing on extended conformation typically show larger $^{3}J_{C'H^{\alpha}}$ values (>2.5 Hz) than the residues found in helical regions of ubiquitin (0.5–2 Hz). The measured couplings were compared with those determined earlier by Wang and Bax using their HCAN[C′] experiment on ubiquitin dissolved in D_2O at pH 4.7 [7]. Comparison of 53 $^{3}J_{C'H^{\alpha}}$ couplings measurable with both experiments gave 0.37 Hz pairwise root mean square deviation (RMSD) (Fig. 3) suggesting precision of ca. 0.2 Hz for the individual measurement. This is in good agreement with the precision of the proposed method. It is noteworthy that largest deviations between the measured couplings and the values provided by Wang and Bax can mostly be found for the residues outside the regular secondary structure of ubiquitin.

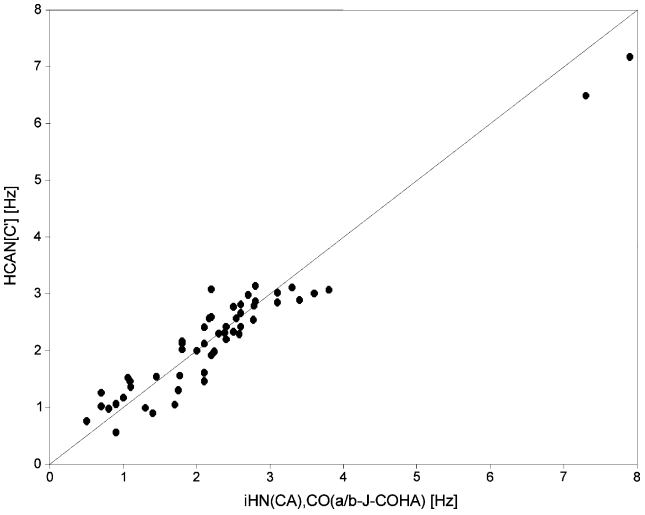

Fig. 3. A pairwise correlation of $^{3}J_{C'H^{\alpha}}$ coupling constants measured from three-dimensional spectrum acquired with the iHN(CA),CO(α/β-*J*-COHA)-TROSY (without active suppression of sequential pathway) vs. ^{3}J couplings measured by Wang and Bax using the HCAN[C′] experiment [7]. The pairwise root-mean-squared deviation between two experiments is 0.37 Hz.

3. Conclusions

In summary, we have introduced novel triple-resonance NMR experiments for measuring $^{3}J_{C'H^{\alpha}}$ scalar couplings in proteins. The proposed iHN(CA),CO(α/β-*J*-COHA) scheme provides precise and sensitive way to measure $^{3}J_{C'H^{\alpha}}$ in two or three-dimensional spectrum with a minimal amount of resonance overlap as was demonstrated on ^{15}N-, ^{13}C-labeled ubiquitin. Alternatively, iHN(CA),CO(α/β-*J*-COHA) scheme with active suppression of sequential pathway or iH(N)CA,CO(α/β-*J*-COHA) experiment with a novel spin-state-selective filter can be employed. The proposed experiments facilitate accurate definition of proteins main chain dihedral ϕ by providing sensitive way to determine $^{3}J_{C'H^{\alpha}}$ as a supplement to routinely measured $^{3}J_{H^{N}H^{\alpha}}$ scalar coupling.

Acknowledgment

This work was supported by the Academy of Finland.

References

[1] M. Karplus, J. Chem. Phys. 30 (1959) 11–15.
[2] V.F. Bystrov, Prog. NMR Spectrosc. 10 (1976) 44–81.
[3] F. Löhr, H. Rüterjans, J. Magn. Reson. 132 (1998) 130–137.
[4] A.C. Wang, A. Bax, J. Am. Chem. Soc. 117 (1995) 1810–1813.
[5] P. Permi, I. Kilpeläinen, A. Annila, J. Magn. Reson. 146 (2000) 255–259.
[6] S. Seip, J. Balbach, H. Kessler, J. Magn. Reson. B 104 (1994) 172–179.
[7] A.C. Wang, A. Bax, J. Am. Chem. Soc. 118 (1996) 2483–2494.
[8] F. Löhr, M. Blümel, J.M. Schmidt, H. Rüterjans, J. Biomol. NMR. 10 (1997) 107–118.
[9] J.-S. Hu, A. Bax, J. Am. Chem. Soc. 118 (1996) 8170–8171.
[10] J.-S. Hu, A. Bax, J. Am. Chem. Soc. 119 (1997) 6360–6368.
[11] A. Bax, G.W. Vuister, S. Grzesiek, F. Delaglio, A.C. Wang, R. Tschudin, G. Zhu, Meth. Enzymol. 239 (1994) 79–105.
[12] F. Löhr, H. Rüterjans, J. Biomol. NMR 13 (1999) 263–274.
[13] A. Rexroth, P. Schmidt, S. Szalma, T. Geppert, H. Schwalbe, C. Griesinger, J. Am. Chem. Soc. 117 (1995) 10389–10390.
[14] A. Meissner, T. Schulte-Herbrüggen, O.W. Sørensen, J. Am. Chem. Soc. 120 (1998) 3803–3804.
[15] F. Löhr, H. Rüterjans, J. Am. Chem. Soc. 119 (1997) 1468–1469.
[16] J.-S. Hu, A. Bax, J. Biomol. NMR 11 (1998) 199–203.
[17] L.E. Kay, A. Bax, J. Magn. Reson. 86 (1990) 110–126.
[18] G. Wagner, P. Schmieder, V. Thanabal, J. Magn. Reson. 93 (1991) 436–440.
[19] M. Billeter, D. Neri, G. Otting, Y.Q. Qian, K. Wüthrich, J. Biomol. NMR 2 (1992) 257–274.
[20] G.W. Vuister, A. Bax, J. Am. Chem. Soc. 115 (1993) 7772–7777.
[21] M. Görlach, M. Wittekind, B.T. Farmer II, L.E. Kay, L. Mueller, J. Magn. Reson. 101 (1993) 194–197.
[22] R. Weisemann, H. Rüterjans, H. Schwalbe, J. Schleucher, W. Bermel, C. Griesinger, J. Biomol. NMR 4 (1994) 231–240.
[23] S. Heikkinen, H. Aitio, P. Permi, R. Folmer, K. Lappalainen, I. Kilpeläinen, J. Magn. Reson. 137 (1999) 243–246.
[24] P. Permi, I. Kilpeläinen, S. Heikkinen, Magn. Res. Chem. 37 (1999) 821.
[25] H. Aitio, P. Permi, J. Magn. Reson. 143 (2000) 391–396.
[26] P. Permi, I. Kilpeläinen, A. Annila, S. Heikkinen, J. Biomol. NMR 16 (2000) 29–37.
[27] A. Petit, S.J.F. Vincent, C. Zwahlen, J. Magn. Reson. 156 (2002) 313–317.
[28] C. Griesinger, O.W. Sørensen, R.R. Ernst, J. Am. Chem. Soc. 107 (1985) 6394–6396.
[29] D. Yang, K. Nagayma, J. Magn. Reson. A 118 (1996) 117–121.
[30] A. Meissner, J.Ø. Duus, O.W. Sørensen, J. Biomol. NMR 10 (1997) 89–94.
[31] P. Andersson, J. Weigelt, G. Otting, J. Biomol. NMR 12 (1998) 435–441.
[32] M. Ottiger, F. Delaglio, A. Bax, J. Magn. Reson. 131 (1998) 373–378.
[33] P. Permi, S. Heikkinen, I. Kilpeläinen, A. Annila, J. Magn. Reson. 140 (1999) 32–40.
[34] P. Permi, P.R. Rosevear, A. Annila, J. Biomol. NMR 17 (2000) 43–54.
[35] P. Permi, J. Biomol. NMR 23 (2002) 201–209.
[36] K. Pervushin, R. Riek, G. Wider, K. Wüthrich, Proc. Natl. Acad. Sci. U.S.A. 94 (1997) 12366–12371.
[37] J.P. Loria, M. Rance, A.G. Palmer III, J. Magn. Reson. 141 (1999) 180–184.
[38] T.M. Logan, E.T. Olejniczak, R.X. Xu, S.W. Fesik, J. Biomol. NMR 3 (1993) 225–231.
[39] B. Brutscher, J. Magn. Reson. 151 (2001) 332–338.
[40] G. Otting, H. Senn, G. Wagner, K. Wütrich, J. Magn. Reson. 70 (1986) 500–505.
[41] D. Marion, M. Ikura, R. Tschudin, A. Bax, J. Magn. Reson. 85 (1989) 393–399.
[42] L.E. Kay, P. Keifer, T. Saarinen, J. Am. Chem. Soc. 114 (1992) 10663–10665.